

# Intracellular Positioning of Isoforms Explains an Unusually Large Adenylate Kinase Gene Family in the Parasite *Trypanosoma brucei*\*<sup>§</sup>

Received for publication, December 8, 2004, and in revised form, January 14, 2005  
Published, JBC Papers in Press, January 18, 2005, DOI 10.1074/jbc.M413821200

Michael L. Ginger,<sup>a,b</sup> E. Solange Ngazoa,<sup>b,c</sup> Claudio A. Pereira,<sup>a,d,e</sup> Timothy J. Pullen,<sup>a</sup>  
Mostafa Kabiri,<sup>f,g</sup> Katja Becker,<sup>c</sup> Keith Gull,<sup>a,h</sup> and Dietmar Steverding<sup>c,f,i,j</sup>

From the <sup>a</sup>Sir William Dunn School of Pathology, University of Oxford, South Parks Road, Oxford, OX1 3RE, United Kingdom, the <sup>b</sup>Interdisziplinäres Forschungszentrum, Justus-Liebig-Universität, Heinrich-Buff-Ring 26–32, 35392 Giessen, Germany, the <sup>c</sup>Instituto de Investigaciones Médicas Alfredo Lanari, Consejo Nacional de Investigaciones Científicas y Técnicas, Universidad de Buenos Aires, Buenos Aires 1427, Argentina, <sup>d</sup>Hygiene-Institut der Ruprecht-Karls-Universität, Im Neuenheimer Feld 324, 69120 Heidelberg, Germany, and the <sup>e</sup>School of Medicine, Health Policy, and Practice, University of East Anglia, Norwich, NR4 7TJ, United Kingdom

Adenylate kinases occur classically as cytoplasmic and mitochondrial enzymes, but the expression of seven adenylate kinases in the flagellated protozoan parasite *Trypanosoma brucei* (order, Kinetoplastida; family, Trypanosomatidae) easily exceeds the number of isoforms previously observed within a single cell and raises questions as to their location and function. We show that a requirement to target adenylate kinase into glycosomes, which are unique kinetoplastid-specific microbodies of the peroxisome class in which many reactions of carbohydrate metabolism are compartmentalized, and two different flagellar structures as well as cytoplasm and mitochondrion explains the expansion of this gene family in trypanosomes. The three isoforms that are selectively built into either the flagellar axoneme or the extra-axonemal paraflagellar rod, which is essential for motility, all contain long N-terminal extensions. Biochemical analysis of the only short form trypanosome adenylate kinase revealed that this enzyme catalyzes phosphotransfer of  $\gamma$ -phosphate from ATP to AMP, CMP, and UMP acceptors; its high activity and specificity toward CMP is likely to reflect an adaptation to very low intracellular cytidine nucleotide pools. Analysis of some of the phosphotransfer network using RNA interference suggests considerable complexity within the homeostasis of cellular energetics. The anchoring of specific adenylate kinases within two distinct flagellar structures pro-

vides a paradigm for metabolic organization and efficiency in other flagellates.

The continuous production of ATP, its delivery from intracellular sites of synthesis to sites of energy consumption, and the homeostasis of adenine nucleotide pools are fundamental to cellular viability. Adenylate kinase (ADK)<sup>1</sup> and phosphagen kinases, such as creatine kinase and arginine kinase, assume pivotal roles in these fundamental processes (1). Phosphagen kinases catalyze reversible phosphotransfer between ATP and the guanidine acceptor (e.g. arginine or creatine), with the phosphagen providing both a temporal and a spatial reserve of high energy phosphate. ADK, on the other hand, catalyzes the transfer of the  $\gamma$ -phosphate group from either ATP or GTP to the phosphoryl acceptor AMP.

Disruption of the single copy ADK gene in *Escherichia coli* or *Schizosaccharomyces pombe* is lethal (2, 3), but in *Saccharomyces cerevisiae* the ADK null phenotype reveals a compensating metabolic plasticity. *S. cerevisiae* survives because the broad substrate specificity of its uridylylase (Ura6p) compensates for the deficiency in cytoplasmic ADK activity (4). However, a small proportion of the yeast ADK (Aky2p) is localized in the mitochondrial intermembrane space (5), where it may contribute to efficient translocation of ATP from the mitochondrial matrix into the cytoplasm (1). Uridylylase is not present in yeast mitochondria, and hence AKY2-deficient *S. cerevisiae* exhibit a petite phenotype and are unable to grow under nonfermentative conditions (6). In skeletal muscle of transgenic AKI<sup>-/-</sup> knock-out mice, metabolic reprogramming and ultrastructural reorganization have been observed (7, 8). Here, glycolytic flux, creatine kinase activity, and mitochondrial volume are increased to support muscle function, albeit with reduced energy economy and efficiency under stress (7–9).

The focus of this study is the uniflagellate protozoan parasite *Trypanosoma brucei*, the causal agent of human African sleeping sickness (see, on the World Wide Web, [www.who.int/tdr/diseases/trypan/](http://www.who.int/tdr/diseases/trypan/)). There are many interesting and unusual aspects to trypanosome metabolism (10). A single aerobically functioning mitochondrion and microbodies of the peroxisome class are present. However, in the mammalian host, the mitochondrial energy metabolism of the parasite is largely re-

\* This work was supported in part by a Wellcome Trust program grant (to K. G., who is a Wellcome Trust Principal Research Fellow), by the Sonderforschungsbereich 544 der Deutschen Forschungsgemeinschaft (to D. S.), The Royal Society (to M. L. G., who is a Royal Society University Research Fellow), by a Forschungsstipendium für Experimentelle Parasitologie der Karl-Enigk-Stiftung (to E. N.), by the fundación Antorchas (to C. A. P.), and by a Biotechnology and Biological Sciences Research Council studentship (to T. J. P.). The costs of publication of this article were defrayed in part by the payment of page charges. This article must therefore be hereby marked "advertisement" in accordance with 18 U.S.C. Section 1734 solely to indicate this fact.

<sup>§</sup> The on-line version of this article (available at <http://www.jbc.org>) contains supplemental data, including an additional table and figure.

<sup>b</sup> Both authors contributed equally to the experimental work.

<sup>c</sup> Supported in Oxford by the Royal Society.

<sup>g</sup> Present address: Aventis Pharma, Mainzer Landstrasse 500, 65795 Hattersheim, Germany.

<sup>h</sup> To whom correspondence may be addressed. Tel.: 44-1865-285455; Fax: 44-1865-285691; E-mail: keith.gull@pathology.oxford.ac.uk.

<sup>j</sup> To whom correspondence may be addressed. Tel.: 44-1603-591291; Fax: 44-1603-593752; E-mail: dsteverding@hotmail.com.

<sup>1</sup> The abbreviations used are: ADK, adenylate kinase; NMPK, nucleotide monophosphate kinase; PFR, paraflagellar rod; RNAi, RNA interference; GFP, green fluorescent protein.

pressed; neither cytochromes nor tricarboxylic acid cycle are present. Glycolysis is the sole energy-generating pathway, and pyruvate is excreted as the major end product of this glucose catabolism. Uniquely, the first seven glycolytic enzymes occur solely in peroxisomes. Peroxisomal targeting of glycolytic enzymes and certain other enzymes utilized for carbohydrate metabolism (10) is characteristic of all trypanosomatids and reflects the description of these trypanosomatid microbodies as glycosomes (10, 11).

*T. brucei* is transmitted between mammalian hosts by its insect vector (*Glossina* sp., tsetse fly). Procyclic trypanosomes (found in the tsetse fly midgut) have an aerobic metabolism and use a variety of carbon sources (12–14), and alternative oxidase and cytochrome *c* oxidase constitute the two terminal enzymes of an essential branched respiratory chain (14, 15). Although oxidative phosphorylation is an important facet of procyclic metabolism, pyruvate kinase and an acetate:succinate CoA-transferase/succinyl-CoA synthetase cycle catalyze important substrate phosphorylations. The cytoplasmic phosphotransfer reaction catalyzed by the former enzyme appears to be essential, except perhaps under conditions where increased substrate availability can result in increased mitochondrial amino acid (proline) metabolism (12, 13, 16). Acetate:succinate CoA transferase is restricted in its evolutionary distribution to trypanosomatid mitochondria, anaerobic helminth mitochondria, and protist hydrogenosomes; it catalyzes formation of acetate from acetyl-CoA. This reaction, rather than entry into the tricarboxylic acid cycle, is the predominant pathway used for acetyl-CoA metabolism; acetate is excreted from the cell as a major end product of metabolism, and the succinyl-CoA product is recycled by mitochondrial succinyl-CoA synthetase, generating ATP (15). Deletion of acetate:succinate CoA-transferase initially results in a severe growth defect, before compensatory metabolic rearrangements allow cells to adapt to loss of the enzyme (17).

Here, we report that the complex stage-regulated metabolism of *T. brucei* is buttressed by the expression of seven ADK-like genes. The expression of seven ADKs within the context of a single cell has not been reported previously, but in this protozoan parasite it reflects the requirement to target ADK into glycosomes and two distinct flagellar structures as well as more classical intracellular sites such as cytoplasm and mitochondrion. Molecular interrogation of the ADK gene family, while demonstrating metabolic adaptation, also indicates that there is likely to be considerable complexity within the relationship between phosphotransfer activity and homeostasis of cellular energetics.

#### MATERIALS AND METHODS

**Reagents**—All chemicals were purchased from Sigma unless otherwise stated. Restriction enzymes and DNA-modifying enzymes were purchased from Roche Applied Science.

**Cells**—Procyclic *T. brucei*, stock 427, was maintained at 27 °C in SDM-79 medium supplemented with 10% (v/v) heat-inactivated fetal calf serum as described previously (18). RNA interference (RNAi) experiments were conducted using the procyclic 29-13 cell line, which has been genetically modified in order to express the tetracycline repressor protein and bacteriophage T7 RNA polymerase (19). Stable integration of exogenous DNA into procyclic cells was carried out as described previously (20). RNAi cell lines were maintained in the presence of the selectable agents hygromycin (50 µg/ml), G-418 (15 µg/ml), and phleomycin (3 µg/ml) until 48 h prior to the start of an experiment. Extracts from long slender and short stumpy bloodstream trypanosomes were prepared and analyzed using antibody markers as described previously (21). Cell counts were determined using either a Neubauer hemocytometer (Sigma), or a CASY1 cell counter (Schärfe System).

**Recombinant DNA Procedures**—Genomic DNA was extracted as described previously (22). RNA was obtained using a High Pure RNA Isolation Kit (Roche Applied Science). Northern and Southern blotting was carried out according to standard protocols (23); blots were washed

to high stringency (0.1× SSC (1× SSC: 0.15 M NaCl, 0.015 M sodium citrate), 0.1% (w/v) SDS; 65 °C). Fluorescein-labeled DNA probes were detected by enhanced chemiluminescence with CDP-star (Amersham Biosciences). For two-step reverse transcription-PCR, cDNA was synthesized using oligo(dT)<sub>15</sub> primer and Omniscript (Qiagen). Incorporation of SyberGreen (Applied Biosystems) into relevant amplicons was determined using an ABI Prism 7700 real time PCR system (Applied Biosystems) and the following thermal cycling parameters: 95 °C, 10 min; 40 cycles of 95 °C, 15 s; 60 °C, 1 min. PCR products were analyzed on gels to confirm the absence of nonspecific amplification. Controls without reverse transcription and amplification using single primers only were also carried out. DNA sequencing was performed using ABI-Prism automated sequencing with custom-designed primers.

**Plasmid Construction**—Detailed descriptions of how the plasmids used in this study were constructed are provided in the supplemental information. RNAi plasmids were based on the opposing promoter system pioneered by Englund and co-workers (20). For immunolocalization of ADKA, ADKB, and ADKE, each containing a single Ty1 epitope at their respective C termini, the plasmids pTAFADKA::Ty, pTAFADKB::Ty, and pTubADKE::Ty were constructed. For the expression of the GFP::ADKD fusion protein, pVsg4GFP::ADKD was constructed. This fusion protein was expressed under the control of an RNA polymerase I-transcribed EP1 promoter following stable integration of pVsg4GFP::ADKD into a minichromosomal locus. For expression of recombinant ADKG in *E. coli*, pTbAKGr was constructed.

**Generation of ADKC<sup>-/-</sup> Null Mutants**—PCR amplification of hygromycin and bleomycin resistance markers was achieved using primer combinations ADKCKo1 and ADKCKo2 (template pGad8-tubulin (24)) or ADKCKo3 and ADKCKo4 (template pRM481 (25)), respectively (see Supplemental Table 1 for primer sequences). The 5' region of each primer contained ~50 bp of homology to the ADKC locus, facilitating gene disruption by homologous recombination; PCR products (3 µg) were used for transformation of procyclic 427 *T. brucei*. For second round transformation of hygromycin-resistant ADKC<sup>-/-</sup> heterozygotes, the bleomycin resistance marker was amplified from a first round heterozygote transformant using a primer combination of ADKCKo5 and ADKCKo6. The resulting PCR product was then used for stable transformation of procyclic cultures. Integration events into trypanosomes were analyzed by PCR and Southern mapping.

**Expression and Analysis of Recombinant ADKG**—Following transformation of pTbAKGr into *E. coli* XL<sub>1</sub>-Blue (Stratagene), expression of recombinant TbADKG was induced by the addition of isopropyl-D-thiogalactopyranoside (60 µg/ml). Recombinant protein was purified by Ni<sup>2+</sup>-nitrilotriacetic acid chromatography according to the manufacturer's protocol (Qiagen). The activity of the recombinant enzyme was measured as described previously by following the rate of NDP formation from NTP and NMP substrates in a coupled system that required pyruvate kinase and lactate dehydrogenase (26). The standard reaction mixture contained Tris-HCl (0.1 M, pH 7.6), KCl (80 mM), MgCl<sub>2</sub> (1.4 mM), phosphoenolpyruvate (400 µM), NADH (200 µM), pyruvate kinase (10 units/ml), lactate dehydrogenase (10 units/ml), NTP (0.8 mM), NMP (2.3 mM), and recombinant ADKG (68.8 µM). One unit of enzyme activity was defined as 1 µmol of NAD<sup>+</sup> formed/min.

**Immunoblotting and Immunofluorescence**—Polyclonal antiserum against recombinant ADKG was prepared by Eurogentech. Polyclonal rabbit antibodies raised against *T. brucei* aldolase were used as described previously (27). SDS-PAGE and immunoblotting were carried out according to standard methods (21). Immunofluorescence of formaldehyde- and methanol-fixed detergent-extracted cytoskeletons using BB2 and ROD-1 (28) monoclonal antibodies was performed as described previously (29, 30).

#### RESULTS

**Seven ADK-like Genes Are Expressed in *T. brucei***—Using NMPK genes characterized from *S. cerevisiae*, *S. pombe*, *Homo sapiens*, *E. coli*, and *Bacillus subtilis* as query sequences, we analyzed the *T. brucei* genome data bases at Sanger and the Institute for Genome Research for the presence of NMPK genes. We found open reading frames homologous to the guanylate kinase and thymidylate kinase from *S. cerevisiae* and humans (31–33), but no hits to cytidylate and uridylate kinase gene families that are unique to bacteria (34–36) (data not shown). We also found a *T. brucei* homologue of a very recently discovered distinct class of ADK genes that is conserved in eukaryotes and Archaea; in *S. cerevisiae* and humans, this novel ADK family member is found in the nucleus (37). How-





TABLE I  
Substrate specificity of *T. brucei* ADKG

Substrates <sup>a</sup>	Activity
	%
AMP/ATP <sup>b</sup>	100
CMP/ATP	225
UMP/ATP	7.5
GMP/ATP	0.1
IMP/ATP	0.3
AMP/CTP	4.7
AMP/UTP	3.7
AMP/GTP	5.6
AMP/ITP	6.5

<sup>a</sup> The substrate concentrations were 2.3 mM NMP and 0.8 mM NTP.

<sup>b</sup> The specific activity of *T. brucei* ADKG with the substrate set of AMP and ATP was 25.9 units/mg of protein and was taken as 100%.

in trypanosomes (more than has ever been observed previously in any other unicellular organism or individual cell type) reflects a molecular radiation to fill particular metabolic niches. Comparison of the trypanosome ADK family with homologues from other organisms indicated that *T. brucei* ADKC and ADKF possess no unusual or structurally distinctive characteristics. In this regard, they resemble the cytoplasmic and mitochondrial ADK isoforms of other eukaryotes. By contrast, our attention was focused by unusual primary sequence characteristics in each of the remaining five *T. brucei* enzymes.

*The Short Form "Cryptic Kinase" Has Broad Substrate Specificity*—TbADKG encodes the only trypanosome short form ADK; the distinction between long and short ADK isoforms referring to the length of the LID domain (38). The LID contributes to the overall folding of NMPKs and changes conformation following the binding of substrate to the enzyme. In mammalian cells, the major cytoplasmic form of ADK is a short form enzyme, and mitochondrial activity is associated with long ADK isoforms (38). In yeast, cytoplasmic and mitochondrial ADK activities are provided by long form ADK enzymes (3, 39). Eukaryotic UMP/CMP kinases share primary sequence homology with ADK and are always of the short kind (38). Careful bioinformatic analysis places ADKG within the UMP/CMP class of NMPK, yet an Asp residue that is predicted to be very important in the discrimination between a CMP/UMP versus an AMP substrate in UMP/CMP kinase (40) is substituted by a Gln residue (Gln<sup>100</sup>) in ADKG. This Gln residue is conserved in the other *T. brucei* ADKs and the previously characterized *S. cerevisiae* proteins Aky2p and Ura6p (Fig. 1), indicating that in ADKG at least one of the residues considered important for catalysis places ADKG with ATP:AMP phosphotransferases rather than UMP/CMP kinases. Ura6p, on the basis of its mutant phenotype, is a UMP/CMP kinase (41) but the presence of Q<sub>111</sub> may contribute to the broad specificity of this enzyme and activity with an AMP substrate (42, 43). We therefore investigated the substrate specificity of the cryptic kinase, ADKG, in more detail.

ADKG was expressed in *E. coli* as a recombinant protein with six His residues at its N terminus and purified using an Ni<sup>2+</sup>-nitrilotriacetic acid column. Following purification, a single protein band of ~24 kDa was visible on a Coomassie Blue-stained SDS-polyacrylamide gel, in close agreement with the predicted molecular mass of 23,793 Da for the recombinant protein (data not shown). The activity of recombinant ADKG with different substrates is shown in Table I. With regard to the phosphate acceptor, ADKG was able to transfer phosphate from ATP to CMP, AMP, and UMP but not to GMP or IMP. The enzyme showed a 30-fold greater substrate preference for CMP relative to UMP and exhibited substantial activity with AMP (44% of that seen for CMP). Using AMP as the acceptor substrate, ATP was found to be the preferred phosphate donor,

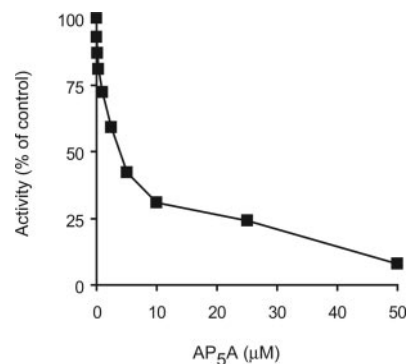


FIG. 2. Inhibition of *T. brucei* adenylate kinase ADKG by diadenosine pentaphosphate. Purified recombinant *T. brucei* ADKG (0.3 μM) was treated with the ADK inhibitor diadenosine pentaphosphate (AP<sub>5</sub>A) for 5 min and then assayed for enzymatic activity under standard conditions with 0.8 mM ATP and 2.3 mM AMP. The ADKG activity is expressed as relative activity (percentage) to untreated control enzyme. Values represent the means of three independent determinations.

although some activity was also seen for other NTP substrates (Table I). ADKG was also inhibited by diadenosine pentaphosphate (AP<sub>5</sub>A in Fig. 2), a transition state analogue that is a specific inhibitor of ADKs but not other NMPKs (44). *K<sub>m</sub>* and *V<sub>max</sub>* values were also calculated (Table II). These indicated that CMP was a higher affinity substrate than AMP. On the other hand, *V<sub>max</sub>* values showed that the enzyme reached similar turnover rates with both AMP and CMP. However, maximum activity with CMP was reached at much lower substrate concentration than with AMP. Immunoblot analysis using polyclonal antibodies raised against recombinant enzyme indicated that a protein band of 24 kDa was present in cell lysates prepared from bloodstream and procyclic trypanosomes (data not shown; gel loading 20 μg of total cell protein from each developmental stage). A lower amount of ADKG was found in the cell cycle-arrested bloodstream stumpy forms (19% of the level seen in long slender pleomorphic AnTat 1.1 bloodstream forms; 28% of the level seen in procyclic trypanosomes) that are preadapted for rapid differentiation into procyclic forms in the tsetse fly midgut, indicating some degree of stage-specific regulation. The homogeneity of such parasite populations was confirmed using antibodies against known stage-regulated proteins, as described previously (21).

*Building ADKs into Two Distinct Flagellar Structures*—To probe the subcellular localization of the three trypanosome ADKs with unusually long leader sequences upstream of the conserved P-loop, we engineered TbADKA, TbADKB, and TbADKE to encode proteins that were tagged at their respective C termini with a single Ty epitope. Recombinant genes were then integrated by homologous recombination into the genome, and expression of the Ty-tagged proteins was determined by immunoblotting and immunofluorescence using the anti-Ty BB2 antibody (29). Immunofluorescence images for ADKA::Ty were reported previously (45) but are also shown here for comparative purposes. On immunoblots a single cross-reactive protein of the expected molecular mass (~30 kDa) was observed only in cell lines expressing a Ty epitope-tagged protein (data not shown). Immunofluorescence signals were also observed only in cells expressing either ADKA::Ty, ADKB::Ty, or ADKE::Ty but not in the untransfected parental cell line, and this signal indicated that each protein was present in the trypanosome flagellum. Importantly, flagellum-associated antibody staining was retained in detergent-extracted trypanosomes (Fig. 3, A–C), indicating that each protein was incorporated into a flagellar cytoskeletal structure. In Fig. 3, A and B, the images shown are of cells double-labeled with the anti-tag



TABLE II  
Kinetic properties of *T. brucei* ADKG

Parameter	Substrate(s)	Value
$K_m$ ( $\mu\text{M}$ )	ATP <sup>a</sup>	0.18
	AMP <sup>b</sup>	3.2
	CMP <sup>b</sup>	0.17
$V_{\text{max}}$ (units/mg)	AMP/ATP	77
	CMP/ATP	78

<sup>a</sup> For  $K_{m(\text{ATP})}$ , the concentration of AMP was fixed at 2.3 mM.

<sup>b</sup> For  $K_{m(\text{NMP})}$ , the concentration of ATP was fixed at 0.18 mM.

antibody BB2 and antibody ROD-1, which detects the paraflagellar rod (PFR), an extra-axonemal structure that runs alongside the classical “9 + 2” axoneme from the point where the flagellum exits the flagellar pocket to its distal tip. Colocalization of the BB2 and ROD-1 antibody patterns indicated, therefore, that ADKA and ADKB are not associated with the axoneme but rather with the PFR. On the other hand, BB2-detected ADKE::Ty did not co-localize with ROD-1 antibody (not shown), and the immunofluorescence extended to a position close to the kinetoplast (Fig. 3C). The kinetoplast is physically attached to the flagellar basal body from which the axoneme extends (46); our immunofluorescence data were therefore consistent with the assembly of an ADK isoform within the trypanosome axoneme. A spectrophotometric enzyme assay confirmed the presence of ADK activity in both cytoskeletal fractions and purified flagella (45).

**Identification of the Glycosomal ADK**—In trypanosomes, ADK activity has been found in purified glycosomes (47–49). The evolutionary connectivity of glycosomes and peroxisomes extends to the conservation of targeting and import mechanisms between both organelles (11). Two canonical recognition signals for the import machinery are a peroxisome targeting signal 1, which is a C-terminal tripeptide motif (typically -SKL), or a peroxisome targeting signal 2, which is a nonapeptide sequence (consensus -(R/K)(L/V/I)X<sub>5</sub>(H/Q)(L/A/F)) at the N-terminal region of the targeted protein. An additional feature of many glycosomal matrix proteins is a high pI. The only gene that we considered likely to encode a glycosomal ADK was *ADKD*; the predicted protein contains a C-terminal -SKL motif and exhibits a pI of 10.1. We demonstrated the glycosomal localization of ADKD through the expression of ADKD, fused at its N terminus to green fluorescent protein (GFP), and colocalization of GFP fluorescence with the glycosomal marker aldolase (Fig. 3D).

**ADKD and ADKF Are Important for Growth**—We used a tetracycline-inducible RNAi system to investigate the consequences of rapidly silencing the expression of each ADK gene in the absence of the longer selective pressure that gene disruption approaches require. Thus, we tracked for up to 14 days post-induction the growth of cell lines in which mRNA for either *ADKA*, *ADKB*, *ADKC*, *ADKD*, *ADKE*, *ADKF*, *ADKG*, or *ADKA* and *ADKB* was specifically targeted for destruction by a double-stranded RNA-mediated decay process. By comparison with the growth rates of noninduced controls, reduced growth was seen only in the case of *ADKD* and *ADKF* knockdowns (Fig. 4). Ultrastructural analysis using electron microscopy indicated that the slow growth phenotype resulting from RNAi against the glycosomal ADK was not accompanied by any obvious change in glycosome morphology or number (data not shown).

Western blot analysis of RNAi cell lines for *ADKG*, encoding a presumably essential UMP/CMP kinase activity, indicated in at least one instance that the absence of phenotype may result from obtaining only a moderate knockdown of protein levels (Supplemental Fig. 1). However, in other cell lines producing no discernable phenotype, an assay of ADK activity in cytoskel-

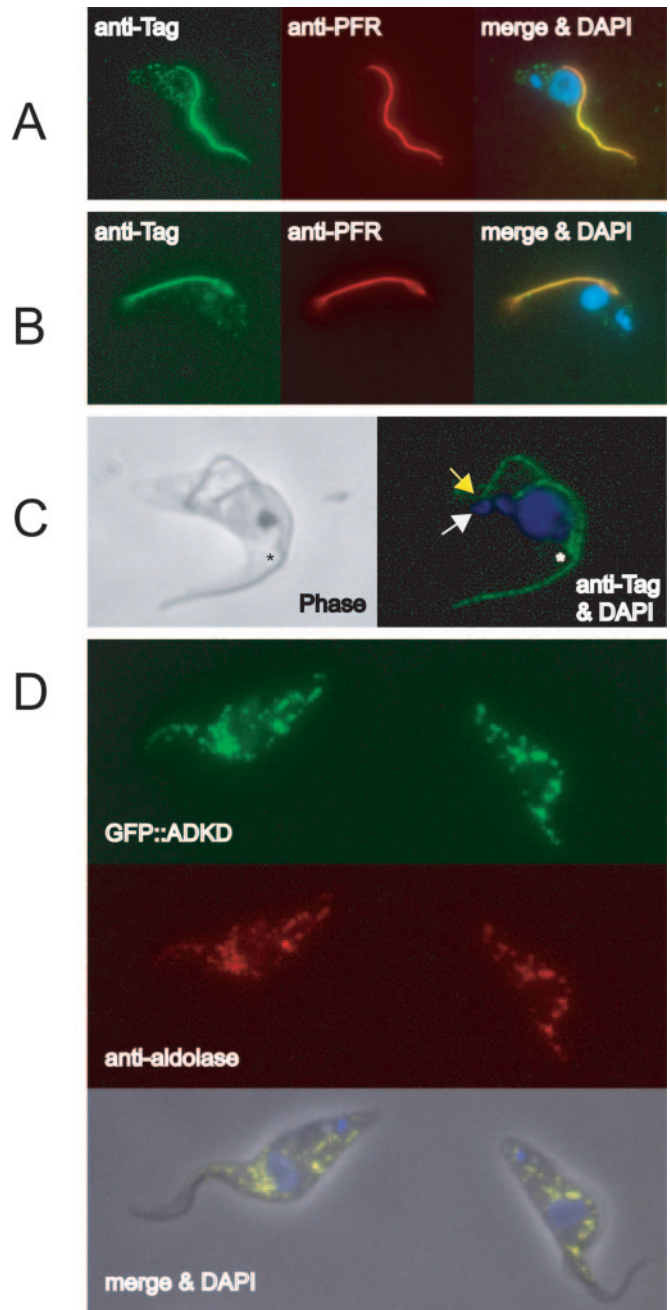
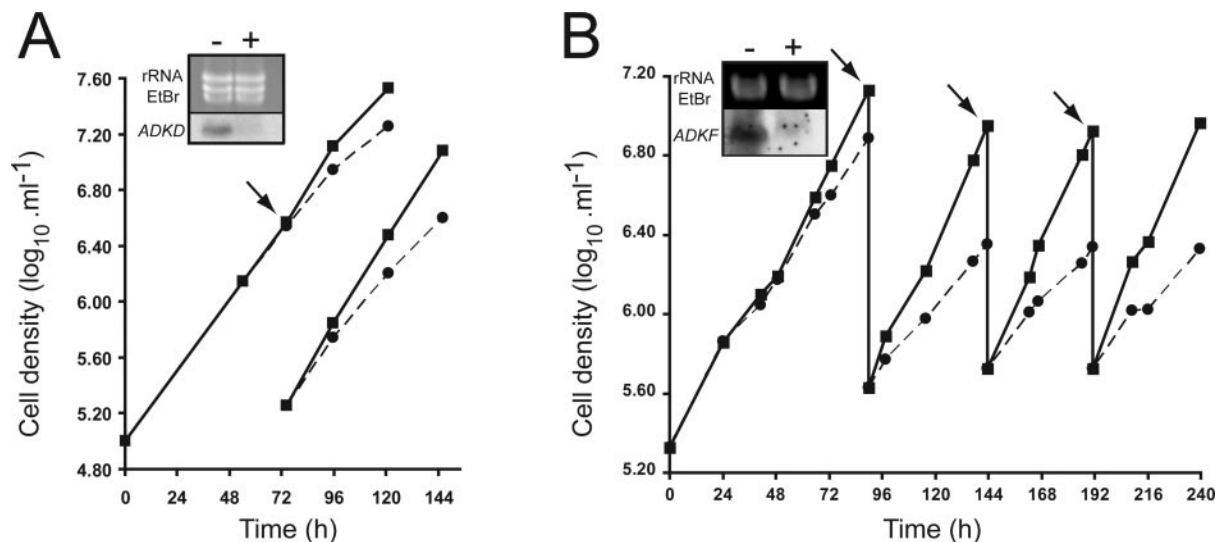


FIG. 3. Localization of ADKA, ADKB, and ADKE to the trypanosome flagellum and ADKD to glycosomes. A and B, detergent-extracted cytoskeletons from cells expressing either ADKA (A) or ADKB (B) proteins tagged at the C terminus with a single Ty epitope were used in double-labeling immunofluorescence with the anti-Ty tag antibody BB2 (anti-Tag; green) and the ROD-1 antibody (anti-PFR; red), which recognizes a minor component of the extra-axonemal paraflagellar rod. 4',6-Diamidino-2-phenylindole-stained nuclei and mitochondrial DNA (kinetoplast) are shown in blue (DAPI). C, immunofluorescence with antibody BB2 of a detergent-extracted cytoskeleton from a cell that was expressing ADKE tagged at the C terminus with a Ty epitope and was also elongating a new flagellum (an asterisk marks the tip of this new flagellum). A white arrowhead shows the position of one kinetoplast, which is physically attached to a flagellar basal body, and the yellow arrowhead indicates the start of an immunofluorescence signal close to this structure. Control experiments using an unmarked procyclic cell line and immunofluorescence using only secondary antibodies confirmed the authenticity of ADKA, ADKB, and ADKE in the trypanosome flagellum. D, co-localization of a GFP::ADKD fusion protein with the glycosomal marker aldolase in immunofluorescence using anti-aldolase-specific antibodies. The merged fluorescence also includes the phase-contrast image.



**FIG. 4. RNAi against either *TbADKD* or *TbADKF* slows growth.** Growth curves are of cells transfected with either p2T7<sup>T3</sup>[ADKD] (A) or p2T7<sup>T3</sup>[ADKF] (B) and incubated in the absence (closed squares, solid lines) or presence (closed circles, dashed lines) of tetracycline (1  $\mu$ g/ml). Shown in the insets are Northern blots (10  $\mu$ g of RNA analyzed per sample) that reveal mRNA abundance for *ADKD* and *ADKF*, respectively, in the absence (-) or presence (+) of tetracycline 24 h after the induction of RNAi. The arrows indicate the points at which cultures were subpassaged to densities shown on each growth curve. Representative experiments using one from a pair of independently obtained stable transformants are shown. Similar experiments carried out with cell lines induced for RNAi against other trypanosome ADK genes or simultaneous RNAi against *TbADKA* and *TbADKB* revealed no significant change in the growth rate relative to the noninduced controls.

etal fractions from the *ADKA* and *ADKB* double knockdown revealed a >80% reduction in activity compared with cytoskeletons isolated from noninduced controls (45). Disruption of the *ADKC* gene produced only very small changes in the doubling time of the *ADKC*<sup>-/-</sup> null mutant (*ADKC*<sup>+/+</sup> 8.12 h versus *ADKC*<sup>+/-</sup> 7.97 h and *ADKC*<sup>-/-</sup> 8.06 h).

**Comparative Genomic Analysis of ADK Families in Trypanosomatids**—Exploiting the recent availability of nearly complete genomic data bases for several trypanosomatid parasites, some of which succeed in environments different from that encountered by *T. brucei*, we asked whether the large ADK gene family identified in the latter species was a common feature of trypanosomatid biology. The results of this survey are summarized in Table III. Based on sequence identity and syntenic conservation, we identified orthologues of *TbADKB*, *ADKC*, *ADKD*, *ADKF*, and *ADKG* from the genomes of *T. cruzi* and *Leishmania major*. Orthologues of *TbADKE* are also present in *T. cruzi*, *L. major*, and *Leishmania infantum*, although intriguingly putative orthologues from both *Leishmania* species are characterized by a series of short deletions (Fig. 5). We also identified a putative ADK isoform that is conserved between *L. major* and *L. infantum* but absent from the *Trypanosoma* genome data bases. Targeting of two distinct ADK isoforms to the PFR appears to be restricted to African trypanosome species (*T. brucei* and *Trypanosoma vivax*).

#### DISCUSSION

Our characterization of the extended ADK gene family in *T. brucei* provides insight into an additional layer of complexity to our understanding of energy metabolism in this important protozoan parasite. Remarkably, the ADK family in trypanosomes is the largest identified so far in any organism; at least seven distinct ADKs are expressed by both bloodstream and procyclic trypanosomes. An obvious question arises as to why the ADK family of trypanosomes is so large. The sequence and distribution within the genome of each ADK gene indicate that this gene family has not arisen as a consequence of recent gene duplication events. Insight into why seven distinct ADKs are needed comes from the revelation that individual isoforms are required in the many diverse cellular compartments that occur in trypanosomes, including its flagellum and the unique glycosomes. A general

absence of introns within protein-coding genes, polycistronic transcription, and a lack of regulation at the level of transcript initiation (50) preclude the use of alternative splicing or alternative transcription start sites to generate the diversity of targeting signals required to partition different products of a single ADK gene between diverse cellular compartments. In other eukaryotic microbes, the use of such molecular mechanisms to differentially target enzymes has been documented (e.g. see Ref. 51). Our attention was focused on those *T. brucei* ADKs with unusual structural properties.

**Substrate Specificity of ADKG**—Sequence analysis of the *T. brucei* ADKs indicated that six enzymes are of the so-called long variety, whereas the seventh enzyme is a short form kinase. Bioinformatic analysis placed this short form enzyme, ADKG, with UMP/CMP kinases of other organisms, but our biochemical analysis of recombinant ADKG revealed that the enzyme was significantly more active using an AMP phosphate acceptor than using UMP. However, it is not without precedent for UMP/CMP kinases to show activity toward AMP; indeed, the yeast orthologue Ura6p has been reported to be more active with an AMP substrate than with CMP (42, 43). Strikingly, the activity of ADKG with CMP is very high (2.5 times the activity seen with AMP) and reaches its  $V_{max}$  at low CMP concentration. We believe this high activity is linked to the very low CTP/CDP pools detected in *T. brucei* (52). The intracellular CTP pool size in *T. brucei* is only 26  $\mu$ M, approximately 10 times lower than the corresponding pool in mouse fibroblasts, and the low  $K_m$  value of ADKG toward CMP may be critical in maintaining CDP/CTP homeostasis. The high catalytic efficiency of *T. brucei* ribonucleotide reductase for CDP reduction and its high affinity for the CDP/UDP-specific effector dATP could also represent biochemical adaptations toward the low CTP pool (53). The broad substrate specificity of ADKG, in particular its activity with AMP, means that we cannot exclude a possibility that this NMPK is multifunctional within the trypanosome cytoplasm.

**ADKs and Cell Fitness**—Slow growth phenotypes were evident following RNAi against *TbADKF* and *TbADKD* in procyclic trypanosomes, but failure to observe growth phenotypes when the expression of other ADKs were subjected to RNAi reflected an inability to completely ablate gene expression



TABLE III  
Distribution of adenylate kinase genes in different trypanosomatids

Gene	Location or function in <i>T. brucei</i>	Homologue in <i>T. cruzi</i>	Homologue in <i>L. major</i>	Homologue in <i>T. vivax</i> <sup>a</sup>
<i>ADKA</i>	Flagellar	No	No	Yes
<i>ADKB</i>	Flagellar	Yes	Yes	Yes
<i>ADKC</i>	ND <sup>b</sup>	Yes	Yes	
<i>ADKD</i>	Glycosomal	Yes	Yes	
<i>ADKE</i>	Flagellar	Yes	Yes	Yes
<i>ADKF</i>	ND	Yes	Yes <sup>c</sup>	
<i>ADKG</i>	UMP/CMP kinase	Yes	Yes	
Other			LmjF25.23702 <sup>d</sup>	

<sup>a</sup> Only the homologues of flagellar enzymes are highlighted.

<sup>b</sup> ND, not determined.

<sup>c</sup> By comparison with homologues in *Trypanosoma*, this protein contains deletions in two *Leishmania* species (Fig. 5).

<sup>d</sup> A homologue is also present in *L. infantum* but is absent from the *Trypanosoma*.

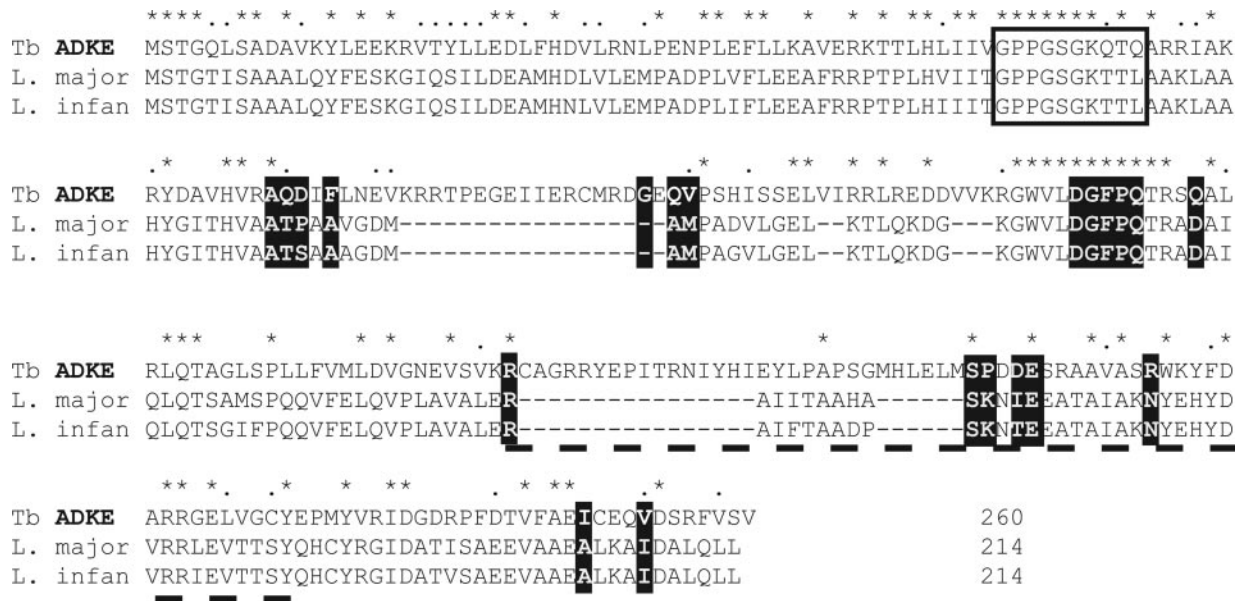


FIG. 5. Primary sequence alignment of ADKE homologues from *T. brucei*, *L. major*, and *L. infantum* highlights deletions within the *Leishmania* proteins. Sequences were initially aligned in Clustal, and then the alignment was adjusted manually. The P-loop is boxed, and the important structural and catalytic residues highlighted in Fig. 1 are shown as white letters on a black background. The asterisks and dots represent residues that are identical or conserved in all three sequences.

(likely in the case of *ADKG*) and/or was suggestive of functional redundancy in culture. Although the notion of metabolic redundancy or flexibility is evident from various molecular interrogations of gene function in trypanosomes (*e.g.* see Refs. 12 and 15), the subtle metabolic restructuring that is observed in transgenic *AK1*<sup>-/-</sup> and *ScCKmit*<sup>-/-</sup>/*IM-CK*<sup>-/-</sup> mice provides a specific paradigm for complex compensatory phenotypes that can arise following the loss of adenylate or creatine kinase activity, respectively (7, 8, 54). Only when tissues were placed under metabolic challenge was the importance of the ADK-catalyzed reaction for muscle function and energetic efficiency realized (7, 9, 55). The ability to observe a mutant phenotype is obviously a consequence of the interrogation conditions; any “no phenotype” statement can merely reflect an inability to apply the correct interrogation conditions.

In the case of the African trypanosome, the niches within which it has evolved (tsetse fly midgut and salivary glands, mammalian bloodstream) are, at present, difficult to interrogate with experimentally tractable cultured parasites. For instance, whereas a classical tricarboxylic acid cycle plays no role in the energy generation of cultured parasites (56), it is not known whether a complete cohort of tricarboxylic acid cycle enzymes is necessary for energy generation at any point during a natural life cycle (14). It is conceivable that maintenance of ATP homeostasis at the lowest metabolic cost could be critical for successful transmission of *T. brucei* through tsetse. In this

context, certain ADKs could therefore assume essential roles that cannot be compensated by an increase in high energy phosphoryl flux through other metabolic pathways. It is perhaps pertinent to note that arginine kinase activity has also been detected in procyclic extracts (57). Again, we have seen that RNAi against *T. brucei* arginine kinase yields no discernable phenotype in culture, although neither arginine kinase activity nor protein can be detected 96 h after induction of RNAi.<sup>2</sup>

Slow growth of the *ADKF* RNAi knockdown indicates loss of a compartmentalized phosphotransfer activity that is not compensable, but we can only speculate as to the cellular role of this isoform. Since we might expect the broad substrate specificity of *ADKG* to be sufficient, at least in culture, to compensate for the loss of any additional cytoplasmic ADK activity, we suggest that slow growth does not occur because of the loss of cytoplasmic *ADKF*. On the other hand, mitochondrial energy generation is critical for growth of procyclic *T. brucei* (12, 15), and in yeast the available data indicate that export of ATP generated in the mitochondrial matrix to the cytoplasm is dependant upon a mitochondrial intermembrane space ADK activity provided by *Aky2p* (4, 6). ADK activity has been detected previously in *T. brucei* mitochondrial fractions (49). By

<sup>2</sup> M. Ginger, C. Pereira, and K. Gull, unpublished results.

analogy with our understanding of yeast biochemistry, further studies could indicate whether ADKF is required for export of mitochondrial ATP in trypanosomes.

**Phosphotransfer within the Flagellum**—In the case of the flagellar ADKs, their independent identification through a proteomic analysis of the trypanosome flagellum (45)<sup>3</sup> and the detection of ADK activity in isolated flagella confirm the localization data presented in this paper. Whereas ADK activity has long been associated with purified eukaryotic flagella (e.g. see Refs. 58 and 59), the identity of *bona fide* flagellar proteins possessing ADK activity had not, until recently, been established. The biological function(s) of such activity remains enigmatic; ADK could contribute to the numerous signaling processes that regulate the coordination of axonemal dynein ATPases and flagellar beating, but equally ADK activity could be required for energetic efficiency within the flagellar compartment. Our discovery of an axonemal *T. brucei* ADK extends our previous identification of ADK in the PFR (45). A parsimonious explanation of such intriguing differential targeting within the flagellum is that ADK assumes a different role depending upon the flagellar structure to which it is targeted.

Integration or positioning within the close proximity of dynein arms is an obvious possibility for any flagellar ADK, and indeed an *ODA5*-dependant association of ADK with outer dynein arms in *Chlamydomonas reinhardtii* was recently reported (60). Intriguingly, however, a survey of the literature indicates that the availability of a flagellar energy-generating pathway may be conserved within flagellates and that the identity of this energy-generating pathway may be determined, at least in part, by the environment in which the flagellum beats. For instance, upon release into sea water, sea urchin spermatozoa derive energy for motility solely from mitochondrial fatty acid oxidation and oxidative phosphorylation; ATP is propagated along the axoneme to the dynein ATPases by a creatine kinase-catalyzed phosphocreatine shuttle (61, 62). On the other hand, within the microaerobic environment of the female reproductive tract, mammalian spermatozoa derive chemical energy from a glycolytic pathway that is compartmentalized through the tethering of hexokinase and glyceraldehyde-3-phosphate dehydrogenase to the fibrous sheath that surrounds the axoneme and outer dense fibers along the principal piece of the sperm tail (63). It is true that sperm are highly polarized cells containing little cytoplasm and perhaps a limited capacity for diffusional exchange of metabolites, but even in the case of a microbial flagellum, the recent characterization of a central pair multiprotein complex containing ADK and enolase subunits highlights the probability of a scaffold for assembly of an energy metabolism within *Chlamydomonas* flagella also (64). In trypanosomes, the first six or seven enzymes of glycolysis are compartmentalized within glycosomes, although we suggest that there is a theoretical possibility that cytoplasmic phosphoglycerate kinase- and pyruvate kinase-catalyzed phosphotransfer could also partition into the flagellum of procyclic trypanosomes. However, during tsetse transmission, glucose is considered to provide a relatively scarce nutrient, with demand for ATP satisfied through the mitochondrial metabolism of amino acid substrates. In this context, the distribution of two ADKs along the length of the PFR could therefore be required to maintain energy economy in much the same way as ADK maintains an essential energy economy in mouse muscle (7, 9). Are trypanosome flagellar ADKs perhaps representative of a more widespread cytoskeletal anchoring of metabolic pathways to maximize energetic efficiency in eukaryotic parasites? Interesting case studies would be flagellate protozoa

*Giardia* and *Trichomonas*; both lack the capacity for oxidative phosphorylation and can rely only on substrate level phosphorylations to generate ATP.

Finally, there is the issue of how ADKs with similar N-terminal extensions are differentially targeted to either axoneme or PFR. We recently demonstrated that PFR targeting of ADKA requires its N-terminal extension (45). Although this N-terminal extension is also sufficient to confer flagellar targeting of GFP, it cannot facilitate detergent- or salt-resistant incorporation of GFP into PFR or axoneme. Anchoring of the ADKs within the trypanosome cytoskeletal architecture therefore requires additional structural elements, and it may be that such features also identify key interacting partners within either axoneme or PFR, respectively.

**Acknowledgments**—We thank Paul Michels (Brussels), Be Wieringa and his group (Nijmegen), Kevin Brindle (Cambridge), León A. Bouvier (Buenos Aires), and Bill Wickstead and Catarina Gadehla (Oxford) for useful discussions during the course of this work; Eleanor Barnwell for technical assistance; and Mike Shaw for electron microscopy. Sequence data for the *T. brucei* genome were obtained from the Institute for Genome Research and the Sanger Institute; sequencing of the *T. brucei* genome was accomplished as part of the *Trypanosoma* Genome Network with support from NIAID, National Institutes of Health, and the Wellcome Trust.

#### REFERENCES

- Dzeja, P. P., and Terzic, A. (2003) *J. Exp. Biol.* **206**, 2039–2047
- Glaser, M., Nulty, W., and Vagelos, P. R. (1975) *J. Bacteriol.* **123**, 128–136
- Konrad, M. (1993) *J. Biol. Chem.* **268**, 11326–11334
- Schricker, R., Magdolen, V., Kaniak, A., Wolf, K., and Bandlow, W. (1992) *Gene (Amst.)* **122**, 111–118
- Strobel, G., Zollner, A., Angermayr, M., and Bandlow, W. (2002) *Mol. Biol. Cell* **13**, 1439–1448
- Bandlow, W., Strobel, G., Zoglowek, C., Oechsner, U., and Magdolen, V. (1988) *Eur. J. Biochem.* **178**, 451–457
- Janssen, E., Dzeja, P. P., Oerlemans, F., Simonetti, A. W., Heerschap, A., de Haan, A., Rush, P. S., Terjung, R. R., Wieringa, B., and Terzic, A. (2000) *EMBO J.* **19**, 6371–6381
- Janssen, E., de Groof, A., Wijers, M., Fransen, J., Dzeja, P. P., Terzic, A., and Wieringa, B. (2003) *J. Biol. Chem.* **278**, 12937–12945
- Pucar, D., Janssen, E., Dzeja, P. P., Juranic, N., Macura, S., Wieringa, B., and Terzic, A. (2000) *J. Biol. Chem.* **275**, 41424–41429
- Hannaert, V., Bringaud, F., Opperdoes, F. R., and Michels, P. A. (2003) *Kinetoplastid Biol. Dis.* **2**, 11
- Moyersoen, J., Choe, J., Fan, E., Hol, W. G., and Michels, P. A. (2004) *FEMS Microbiol. Rev.* **28**, 603–643
- Coustou, V., Besteiro, S., Biran, M., Dirolez, P., Bouchaud, V., Voisin, P., Michels, P. A., Canioni, P., Baltz, T., and Bringaud, F. (2003) *J. Biol. Chem.* **278**, 49625–49635
- ter Kuile, B. H. (1997) *J. Bacteriol.* **179**, 4699–4705
- van Weelden, S. W., Fast, B., Vogt, A., van der Meer, P., Saas, J., van Hellemond, J. J., Tielens, A. G., and Boshart, M. (2003) *J. Biol. Chem.* **278**, 12854–12863
- Bochud-Allemann, N., and Schneider, A. (2002) *J. Biol. Chem.* **277**, 32849–32854
- Morris, J. C., Wang, Z., Drew, M. E., and Englund, P. T. (2002) *EMBO J.* **21**, 4429–4438
- Riviere, L., Van Weelden, S. W., Glass, P., Vegh, P., Coustou, V., Biran, M., Van Hellemond, J. J., Bringaud, F., Tielens, A. G., and Boshart, M. (2004) *J. Biol. Chem.* **279**, 45337–45346
- Brun, R., and Schonenberger, (1979) *Acta Trop.* **36**, 289–292
- Wirtz, E., Leal, S., Ochatt, C., and Cross, G. A. (1999) *Mol. Biochem. Parasitol.* **99**, 89–101
- Wang, Z., Morris, J. C., Drew, M. E., and Englund, P. T. (2000) *J. Biol. Chem.* **275**, 40174–40179
- Breidbach, T., Krauth-Siegel, R. L., and Steverding, D. (2000) *FEBS Lett.* **473**, 212–216
- Bernards, A., Van der Ploeg, L. H., Frasch, A. C., Borst, P., Boothroyd, J. C., Coleman, S., and Cross, G. A. (1981) *Cell* **27**, 497–505
- Sambrook, J., Fritsch, E. F., and Maniatis, T. (1989) *Molecular Cloning: A Laboratory Manual*, 2nd Ed., Cold Spring Harbor Laboratory Press, Cold Spring Harbor, NY
- Wickstead, B., Ersfeld, K., and Gull, K. (2003) *Nucleic Acids Res.* **31**, 3993–4000
- Conway, C., Proudfoot, C., Burton, P., Barry, J. D., and McCulloch, R. (2002) *Mol. Microbiol.* **45**, 1687–1700
- Berghausen, J. (1975) *Biochim. Biophys. Acta* **397**, 370–376
- Lorenz, P., Maier, A. G., Baumgart, E., Erdmann, R., and Clayton, C. (1998) *EMBO J.* **17**, 3542–3555
- Woods, A., Sherwin, T., Sasse, R., MacRae, T. H., Baines, A. J., and Gull, K. (1989) *J. Cell Sci.* **93**, 491–500
- Bastin, P., Bagherzadeh, Z., Matthews, K. R., and Gull, K. (1996) *Mol. Biochem. Parasitol.* **77**, 235–239
- Bastin, P., Pullen, T. J., Sherwin, T., and Gull, K. (1999) *J. Cell Sci.* **112**, 3769–3777

<sup>3</sup> K. Gull, unpublished results.



31. Jong, A. Y., Kuo, C. L., and Campbell, J. L. (1984) *J. Biol. Chem.* **259**, 11052–11059
32. Su, J. Y., and Sclafani, R. A. (1991) *Nucleic Acids Res.* **19**, 823–827
33. Konrad, M. (1992) *J. Biol. Chem.* **267**, 25652–25655
34. Bucurenci, N., Sakamoto, H., Briozzo, P., Palibroda, N., Serina, L., Sarfati, R. S., Labesse, G., Briand, G., Danchin, A., Barzu, O., and Gilles, A. M. (1996) *J. Biol. Chem.* **271**, 2856–2862
35. Schultz, C. P., Ylisastigui-Pons, L., Serina, L., Sakamoto, H., Mantsch, H. H., Neuhard, J., Barzu, O., and Gilles, A. M. (1997) *Arch. Biochem. Biophys.* **340**, 144–153
36. Serina, L., Blondin, C., Krin, E., Sismeyro, O., Danchin, A., Sakamoto, H., Gilles, A. M., and Barzu, O. (1995) *Biochemistry* **34**, 5066–5074
37. Ren, H., Wang, L., Bennett, M., Liang, Y., Zheng, X., Lu, F., Li, L., Nan, J., Luo, M., Eriksson, S., Zhang, C., and Su, X. D. (2005) *Proc. Natl. Acad. Sci. U. S. A.*, **102**, 303–308
38. Fukami-Kobayashi, K., Nosaka, M., Nakazawa, A., and Go, M. (1996) *FEBS Lett.* **385**, 214–220
39. Konrad, M. (1988) *J. Biol. Chem.* **263**, 19468–19474
40. Scheffzek, K., Kliche, W., Wiesmuller, L., and Reinstein, J. (1996) *Biochemistry* **35**, 9716–9727
41. Liljelund, P., and Lacroute, F. (1986) *Mol. Gen. Genet.* **205**, 74–81
42. Muller-Dieckmann, H. J., and Schulz, G. E. (1995) *J. Mol. Biol.* **246**, 522–530
43. Muller-Dieckmann, H. J., and Schulz, G. E. (1994) *J. Mol. Biol.* **236**, 361–367
44. Feldhau, P., Frohlich, T., Goody, R. S., Isakov, M., and Schirmer, R. H. (1975) *Eur. J. Biochem.* **57**, 197–204
45. Pullen, T. J., Ginger, M. L., Gaskell, S. J., and Gull, K. (2004) *Mol. Biol. Cell* **15**, 3257–3265
46. Ogbadoyi, E. O., Robinson, D. R., and Gull, K. (2003) *Mol. Biol. Cell* **14**, 1769–1779
47. Hart, D. T., Misset, O., Edwards, S. W., and Opperdoes, F. R. (1984) *Mol. Biochem. Parasitol.* **12**, 25–35
48. McLaughlin, J. (1985) *Mol. Biochem. Parasitol.* **14**, 219–230
49. Opperdoes, F. R., Markos, A., and Steiger, R. F. (1981) *Mol. Biochem. Parasitol.* **4**, 291–309
50. Clayton, C. E. (2002) *EMBO J.* **21**, 1881–1888
51. Szcwecyk, E., Andrianopoulos, A., Davis, M. A., and Hynes, M. J. (2001) *J. Biol. Chem.* **276**, 37722–37729
52. Hofer, A., Steverding, D., Chabes, A., Brun, R., and Thelander, L. (2001) *Proc. Natl. Acad. Sci. U. S. A.* **98**, 6412–6416
53. Hofer, A., Ekanem, J. T., and Thelander, L. (1998) *J. Biol. Chem.* **273**, 34098–34104
54. Steeghs, K., Oerlemans, F., de Haan, A., Heerschap, A., Verdoodt, L., de Bie, M., Ruitenbeek, W., Benders, A., Jost, C., van Deursen, J., Tullson, P., Terjung, R., Jap, P., Jacob, W., Pette, D., and Wieringa, B. (1998) *Mol. Cell. Biochem.* **184**, 183–194
55. Steeghs, K., Benders, A., Oerlemans, F., de Haan, A., Heerschap, A., Ruitenbeek, W., Jost, C., van Deursen, J., Perryman, B., Pette, D., Bruckwilder, M., Koudijs, J., Jap, P., Veerkamp, J., and Wieringa, B. (1997) *Cell* **89**, 93–103
56. van Weelden, S. W., van Hellemond, J. J., Opperdoes, F. R., and Tielsen, A. G. (January 12, 2005) *J. Biol. Chem.* 10.1074/jbc.M412447200
57. Pereira, C. A., Alonso, G. D., Torres, H. N., and Flawia, M. M. (2002) *J. Eukaryot. Microbiol.* **49**, 82–85
58. Watanabe, T., and Flavin, M. (1976) *J. Biol. Chem.* **251**, 182–192
59. Schoff, P. K., Cheetham, J., and Lardy, H. A. (1989) *J. Biol. Chem.* **264**, 6086–6091
60. Wirschell, M., Pazour, G., Yoda, A., Hirono, M., Kamiya, R., and Witman, G. B. (2004) *Mol. Biol. Cell* **15**, 2729–2741
61. Tombes, R. M., and Shapiro, B. M. (1985) *Cell* **41**, 325–334
62. Kaldis, P., Stolz, M., Wyss, M., Zanolla, E., Rothen-Rutishauser, B., Vorherr, T., and Wallimann, T. (1996) *J. Cell Sci.* **109**, 2079–2088
63. Miki, K., Qu, W., Goulding, E. H., Willis, W. D., Bunch, D. O., Strader, L. F., Perreault, S. D., Eddy, E. M., and O'Brien, D. A. (2004) *Proc. Natl. Acad. Sci. U. S. A.* **101**, 16501–16506
64. Zhang, H., and Mitchell, D. R. (2004) *J. Cell Sci.* **117**, 4179–4188